Role of the Active Site Cysteine of DpgA, a Bacterial Type III Polyketide Synthase†

Claire C. Tseng,‡ Shaun M. McLoughlin,§ Neil L. Kelleher,§ and Christopher T. Walsh*,‡

Department of Biological Chemistry and Molecular Pharmacology, Harvard Medical School, 240 Longwood Avenue, Boston, Massachusetts 02115, and Department of Chemistry, University of Illinois at Urbana-Champaign, 600 South Mathews Avenue, Urbana, Illinois 61801

Received September 23, 2003; Revised Manuscript Received November 21, 2003

ABSTRACT: DpgA is a bacterial type III polyketide synthase (PKS) that decarboxylates and condenses four malonyl-CoA molecules to produce 3,5-dihydroxyphenylacetyl-CoA (DPA-CoA) in the biosynthetic pathway to 3,5-dihydroxyphenylglycine, a key nonproteinogenic residue in the vancomycin family of antibiotics. DpgA has the conserved catalytic triad of Cys/His/Asn typical of type III PKS enzymes, and has been assumed to use Cys160 as the catalytic nucleophile to create a series of elongating acyl-*S*-enzyme intermediates prior to the C_8 to C_3 cyclization step. Incubation of purified DpgA with [^{14}C]-malonyl-CoA followed by acid quench during turnover leads to accumulation of 10−15% of the DpgA molecules covalently acylated. Mutation of the active site Cys160 to Ala abrogated detectable covalent acylation, but the C160A mutant retained 50% of the V_{max} for DPA-CoA formation, with a k_{cat} still at 0.5 catalytic turnovers/min. For comparison, a C190A mutant retained wild-type activity, while the H296A mutant, in which the side chain of the presumed catalytic His is removed, had a 6-fold drop in k_{cat}. During turnover, purified DpgA produced 1.2 equivalents of acetyl-CoA for each DPA-CoA, indicating 23% uncoupled decarboxylation competing with condensative C−C coupling. The C160A mutant showed an increased partition ratio for malonyl-CoA decarboxylation to acetyl-CoA vs condensation to DPA-CoA, reflecting more uncoupling in the mutant enzyme. The Cys-to-Ala mutant thus shows the unexpected result that, when the normal acyl-*S*-enzyme mechanism for this type III PKS elongation/cyclization catalyst is removed, it can still carry out the regioselective construction of the eight-carbon DPA-CoA skeleton with surprising efficiency.

In the biosynthesis of the vancomycin and teicoplanin family of glycopeptide antibiotics [including chloroeremomycin (*1*), balhimycin (*2*), complestatin (*3*), A40926 (*4*), and A47934 (*5*)], the relevant biosynthetic genes are clustered for coordinate transcriptional regulation of all of the proteins required for antibiotic production (*6*). The gene clusters include the multimodular nonribosomal peptide synthetase (NRPS)[1] subunits responsible for the thiotemplate assembly of the heptapeptide core via a cascade of elongating acyl-*S*-pantetheinyl enzyme intermediates (*7*). They also typically include tailoring enzymes (*8*), such as *N*-methylases, oxidative cross-linking heme proteins, glycosyl transferases (Gtfs), and enzymes for creating the TDP-aminodeoxy sugar substrates for the Gtfs.

A hallmark of many nonribosomal peptides, and of the vancomycin/teicoplanin group in particular, are nonproteinogenic amino acid residues. Notably, 4-hydroxyphenylglycine (Hpg) and 3,5-dihydroxyphenylglycine (Dpg) are found at three of the seven positions (residues 4/5/7) of the heptapeptide scaffold of vancomycin and at five of the seven positions (residues 1/3/4/5/7) of teicoplanin (Figure 1a). These residues are involved in the post-assembly line oxidative cross-linking that generates the cup-shaped architecture necessary for target recognition by these antibiotics (*9*). The Hpg and Dpg monomers are made from primary metabolites on a "just in time" basis by including their biosynthetic genes in the vancomycin and teicoplanin clusters.

While Hpg is made by a four enzyme sequence from chorismate, the primary intermediate for aromatic amino acid biosynthesis (*10*, *11*), streptomycetes and actinomycetes make the eight-carbon skeleton of the aromatic amino acid Dpg by polyketide logic. A four gene operon, *dpgA-D*, encodes enzymes that convert four malonyl-CoA molecules to 3,5-dihydroxyphenylglyoxylate (DPGx), a transamination away from Dpg (*12*, *13*). Initial studies with *Amycolatopsis mediterranei* genes expressed in *Streptomyces lividans* (*12*), and with *Amycolatopsis orientalis* DpgA-D overproduced and purified in *Escherichia coli* (*13*), established the outline of the biosynthetic logic (Figure 1b). DpgA is a type III polyketide synthase (PKS), taking four molecules of malonyl-CoA to 3,5-dihydroxyphenylacetyl-CoA (DPA-CoA, Scheme 1). The rate of formation of this eight-carbon aryl-CoA is

† This work was supported by National Institutes of Health Grants GM 49338 (C.T.W.) and GM 067725 (N.L.K.). C.C.T. is a National Defense Science and Engineering Graduate Fellow.

* To whom correspondence should be addressed. Phone: (617) 432-1715. Fax: (617) 432-0438. E-mail: christopher_walsh@hms.harvard.edu.

‡ Harvard Medical School.

§ University of Illinois at Urbana-Champaign.

[1] Abbreviations: DPA-CoA, 3,5-dihydroxyphenylacetyl-CoA; Dpg, 3,5-dihydroxyphenylglycine; DPGx, 3,5-dihydroxyphenylglyoxylate; Hpg, 4-hydroxyphenylglycine; NRPS, nonribosomal peptide synthetase; PKS, polyketide synthase.

10.1021/bi035714b CCC: $27.50
Published on Web 01/08/2004

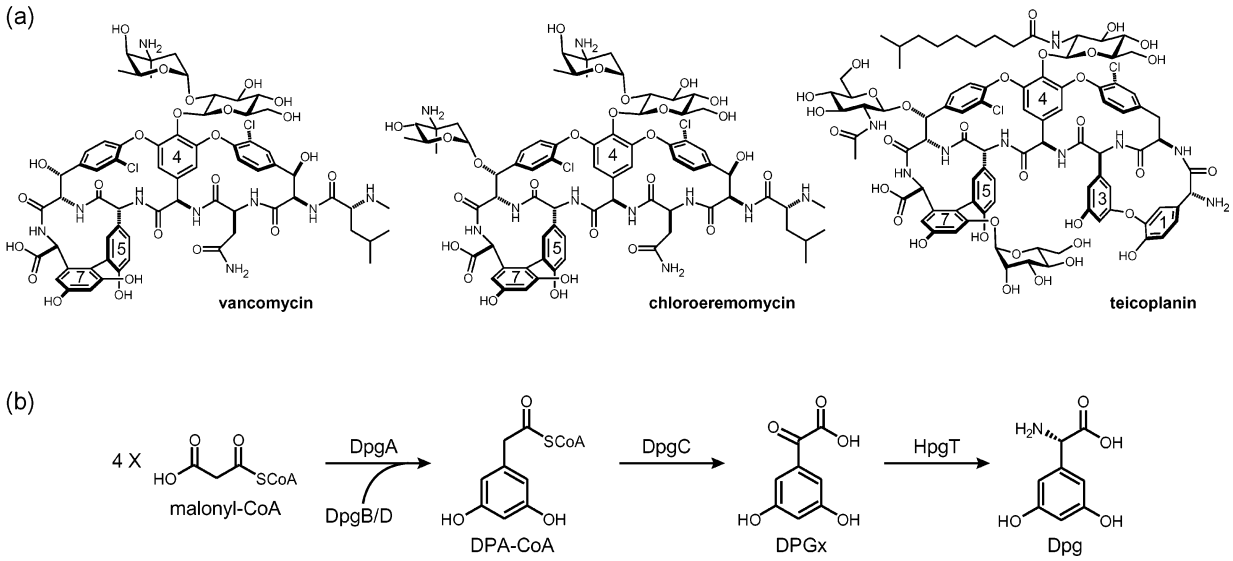

FIGURE 1: (a) Glycopeptide antibiotics containing the nonproteinogenic amino acids Dpg and Hpg. The Dpg and Hpg residues in each structure are indicated by their residue numbers. (b) Scheme of biosynthetic pathway of Dpg.

Scheme 1: Proposed Mechanism of Action of DpgA[a]

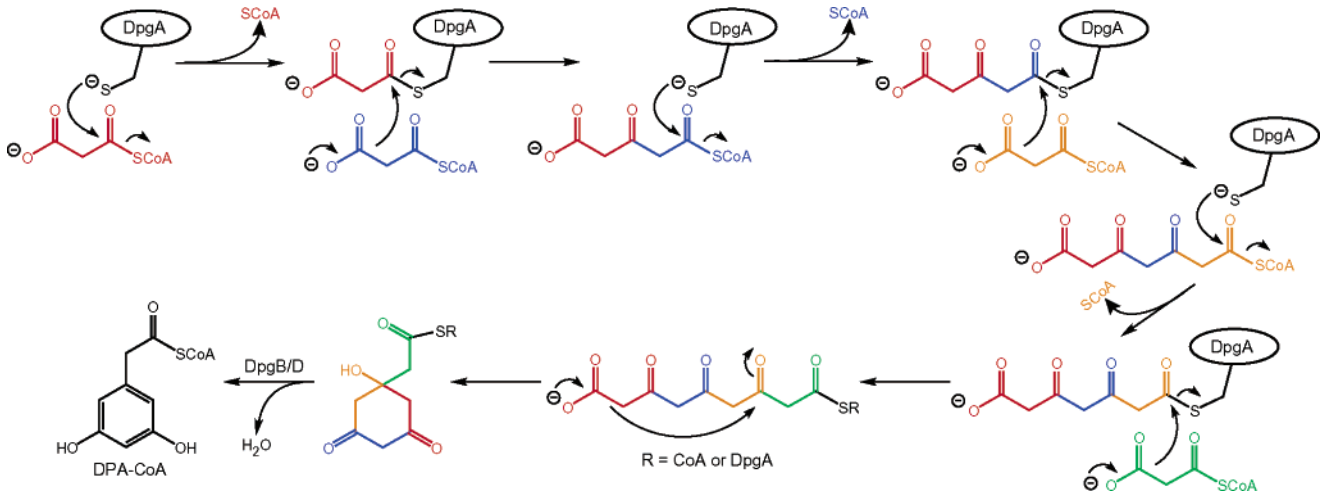

[a] Each of the four malonyl-CoA substrates is indicated by a unique color.

accelerated 35-fold by the addition of DpgB and DpgD, which likely dehydrate the initial cyclic precursor to DPA-CoA, perhaps while still bound to DpgA (*13*). Then, DpgC, a surprising metal- and redox cofactor-independent oxygenase, cleaves the thioester while carrying out a four-electron oxidation of the benzylic CH_2 group of DPA-CoA to the keto group of DPGx by an as yet undetermined mechanism (*13*) (Figure 1b).

In this study, we focus on the type III PKS enzyme, DpgA. Type III PKSs are biosynthetic enzymes found in plants and bacteria, with chalcone synthase the prototypical member (*14*). The first characterized bacterial type III PKS was RppA, which synthesizes 1,3,6,8-tetrahydroxynaphthalene from five decarboxylative condensations of malonyl-CoA, followed by cyclization and aromatization (*15*). A conserved catalytic triad consisting of Cys, His, and Asn is required for this multistep activity (*14*).

Here we investigate the mechanism of action of DpgA, which has similar substrate specificity to RppA (using malonyl-CoA as both starter and extender unit), but catalyzes one less condensation and has a different regioselectivity of cyclization. We analyze the degree of uncoupling of malonyl-CoA decarboxylation (to unproductive acetyl-CoA) vs productive C−C bond formation, as well as the amount of enzyme that accumulates as covalent acyl-*S*-Cys-enzyme forms during turnover. Surprisingly, mutation of the catalytic Cys to the nonnucleophilic side chain of Ala only lowered DPA-CoA formation rates by 50%, although it did lower covalent acyl-enzyme species to undetectable levels. Analogously, mutation of the conserved catalytic His reduced DpgA rate of product formation only an order of magnitude. Implications for the catalytic mechanism of this type III PKS enzyme are discussed.

EXPERIMENTAL PROCEDURES

Materials. Oligonucleotide primers were purchased from Integrated DNA Technologies. Restriction enzymes and T4 DNA ligase were purchased from New England Biolabs. Plasmid vectors were purchased from Novagen. Pfu polymerase and competent *E. coli* were purchased from Stratagene. Isopropyl β-D-thiogalactopyranoside (IPTG) was purchased from Research Products International. [2-^{14}C]-Malonyl-CoA was purchased from New England Nuclear. All other chemicals were purchased from Sigma-Aldrich.

Table 1: DNA Primer Pairs Used in Construction of DpgA Mutants

mutant	primer pairs[a]
C160A	DpgANterm: 5′-GGGAATTCCATATGGGGGTGGATGTATCGATGACG-3′
	C160Arev: 5′-GTTCAGGCCGGCGTT**GGC**GCCCATGCCAACGATG-3′
	C160Afor: 5′-CATCGTTGGCATGGGC**GCC**AACGCCGGCCTGAAC-3′
	DpgACterm: 5′-AGCTTTGAATTCTCACCATTGGATCAGCGCCATTT-3′
C160S	DpgANterm
	C160Srev: 5′-CGTTCAGGCCGGCGTT**CGA**ACCCATGCCAACGATG-3′
	C160Sfor: 5′-CATCGTTGGCATGGGT**TCG**AACGCCGGCCTGAACG-3′
	DpgACterm
H296A	DpgANterm
	H296Arev: 5′-CTTCTTGCCGCCTGA**GGC**CACCAGCCAATGGCCG-3′
	H296Afor: 5′-CGGCCATTGGCTGGTG**GCC**TCAGGCGGCAAGAAG-3′
	DpgACterm
C190A	DpgANterm
	C190Arev: 5′-GGGCGTAAGCGGCGCT**AGC**CGCCTCGCTGCACAGG-3′
	C190Afor: 5′-CCTGTGCAGCGAGGCG**GCT**AGCGCCGCTTACCGCC-3′
	DpgACterm

[a] Codon of introduced point mutation in bold; introduced restriction site underlined.

Construction of DpgA Mutants. The C160A, C160S, H296A, and C190A mutants were created by sequence overlap extension (SOE) mutagenesis (*16*) of the plasmid containing wild-type DpgA (*13*), using the primers listed in Table 1. The codon for the mutation was chosen such that a unique restriction site was introduced, to facilitate the use of diagnostic digests to confirm the introduction of the mutation. For the C160S, H296A, and C190A mutants, the introduction of such a restriction site required additional basepair changes that resulted in a silent mutation. The C160A/H296A double mutant was created by SOE mutagenesis of the plasmid containing the C160A mutant, using the primers for creating the H296A mutant. All of the mutants were cloned into the *Nde* I/*Eco*R I sites of the pET-16b vector, which encodes an N-terminal His_{10}-tag. The identities of all of the mutants were verified by DNA sequencing at the Molecular Biology Core Facilities of the Dana Farber Cancer Institute (Boston, MA).

Overexpression and Purification. Wild-type DpgA, DpgB, and DpgD were overexpressed and purified from *E. coli* BL21(DE3) as previously described (*13*). DpgA mutants were overexpressed and purified following the same procedure, except that cultures were grown at 24 °C until mid-log phase and then grown at 15 °C overnight after IPTG induction. Proteins were dialyzed into 25 mM Tris-HCl, pH 7.5/100 mM NaCl/15% glycerol/1 mM DTT, flash frozen, and stored at −80 °C.

Fourier Transform Mass Spectrometry (FTMS). One-hundred-microliter aliquots of wild-type DpgA (59 μM) and the C160A (14 μM) and C160S (60 μM) mutants were injected onto a Jupiter C4 reverse phase column. After extensive washing in 90% water, the protein was eluted in 90% acetonitrile. The subsequent sample was lyophilized and resuspended in 40 μL of electrospray solution (78% acetonitrile, 20% water, 2% acetic acid). The protein was directly infused into a custom-built quadrupole-FTMS hybrid instrument through a microelectrospray assembly terminated with a 50-μm inner diameter ESI tip. The resulting ions were passed through a resistively heated metal capillary and skimmer before being externally accumulated for a total of 4 s in an accumulation octapole (*17*). After accumulation, the ions were shuttled to the ICR cell via an rf-only transfer octapole.

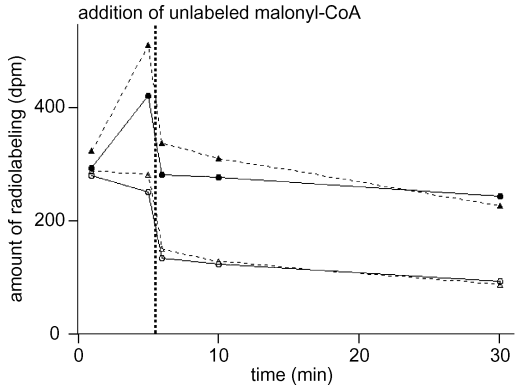

FIGURE 2: Time courses of unlabeled malonyl-CoA chase of [^{14}C]-malonyl-CoA label on wild-type DpgA and the C190A mutant. Filled circle: DpgA wt; filled triangle: DpgA C190A; open circle: DpgA wt + DpgB/DpgD; open triangle: DpgA C190A + DpgB/DpgD. Reaction conditions are as described in Materials and Methods. 40% of incorporated label is chased in the absence of DpgB and DpgD, and 80% is chased in the presence. Data shown are representative of time courses performed in triplicate. The amount of variation among separate time courses was less than 10%, and the background rate of radiolabeling in the absence of enzyme was less than 40 dpm.

The resulting spectra showed that the relative molecular weight (M_r) within five parts-per-million (ppm) of wild-type DpgA after 150 scans was 41927.3-*0* Da, which is consistent with the DNA-predicted sequence of DpgA without the start Met residue (Figure 4b). Further, the primary sequence of wild-type DpgA was extensively verified by cyanogen bromide digestion and molecular weight verification for six peptides within 20 ppm. This peptide mapping procedure verified 90% of the primary sequence of DpgA (data not shown). The M_r values of the C160S and C160A mutants were also consistent with their sequences: 41909.6-*0* Da (36 ppm, 100 scans) and 41895.5-*0* (10 ppm, 100 scans), respectively (Figure 4c,d). The values reported in this study are monoisotopic molecular weights as indicated by the italicized zero after the M_r values (*18*).

Radiolabeling Assays. Incubations of DpgA/DpgB/DpgD with [^{14}C]-malonyl-CoA for HPLC detection of radiolabeled products were performed, worked up, and analyzed as previously described (*13*). For time courses, [^{14}C]-malonyl-CoA (3 μM, 0.87 Ci/mol) was incubated with wild-type or mutant DpgA (0.6 μM) either in the presence or absence of

```
DpgA   150   CSRSDIVGMGCNAGLNALNVVAGWSAAHPGELGVVLCSEACSAAY--ALDGTMRTAVVNSLFGDGSAALAVISGDRRVPGP
RppA   128   TRQLPIAQLGCAAGGAAINRAHDFCVAYPDSNVLIVSCEFCSLCYQ-PTDIGVGSLLSNGLFGDALSAAVV----RGQG-G
PhlD   128   TVQLPIAQLGCVAGAAAINRANDFASLSPDNHALIVSLEFSSLCYQ-PQDTKLHAFISAALFGDAVSACVM----RADDKA
2-PS   159   VKRYMLYQQGCAAGGTVLRLAKDLAENNKGSRVLIVCSEITAILFHGPNENHLDSLVAQALFGDGAAALIVGSGPHLAVER
CHS    154   VKRYMMYQQGCFAGGTVLRLAKDLAENNKGARVLVVCSEVTAVTFRGPSDTHLDSLVGQALFGDGAAALIVGSDPVPEIEK

DpgA   229   RVLKFAS---YIITDAVDAMRYDWDRDQDRFSFFLDPQIPYVVGAHAEIVINRL--LSGTGLRRSDIGHWLVHSGGKKVVD
RppA   203   TGMRLERNGSHLVPDTEDWISYAV-RDTG-FHFQLDKRVPGTM-EMLAPVLLDLVDLHGWSV--PNMDFFIVHAGGPRILD
PhlD   204   PGFKIAKTGSYFLPDSEHYIKYDV-KDSG-FHFTLDKAVMNSI-KDVAPMMEEL-NFETFNQHCAQNDFFIFHTGGRKILD
2-PS   240   PIFEIVSTDQTILPDTEKAMKLHL-REGG-LTFQLHRDVPLMVAKNIENAAEK--ALSPLGITDWNSVFWMVHPGGRAILD
CHS    235   PIFEMVWTAQTIAPDSEGAIDGHL-REAG-LTFHLLKDVPGIVSKNINKALVE--AFEPLGISDYNSIFWIAHPGGPAILD

DpgA   305   AVVVNLGLSRHDVRHTTGVLRDYGNLSSGSFLFSY
RppA   279   DLCHFLDLPPEMFRYSRATLTERGNIASSVVF---
PhlD   281   ELVLQLDLEPGRVAQSRDSLSEAGNIASVVVF---
2-PS   317   QVERKLNLKEDKLRASRHVLSEYGNLISACVLFII
CHS    312   QVEQKLALKPEKMKATREVLSEYGNMSSACVLFIL
```

FIGURE 3: Sequence alignment of DpgA with other bacterial and plant type III PKSs. RppA, *Streptomyces griseus* 1,3,6,8-tetra-hydroxynaphthalene synthase, accession BAA33495; PhlD, *Pseudomonas fluorescens* monoacetylphloroglucinol synthase, accession AAB48106; 2-PS, *Gerbera hybrida* methylpyrone synthase, accession CAA86219; CHS, *Medicago sativa* chalcone synthase, accession P30074. Catalytic triad residues (Cys160, His296, Asn329 in DpgA) are indicated by asterisks; an additional Cys residue predicted to be in the DpgA active site (Cys190) is indicated by an arrow.

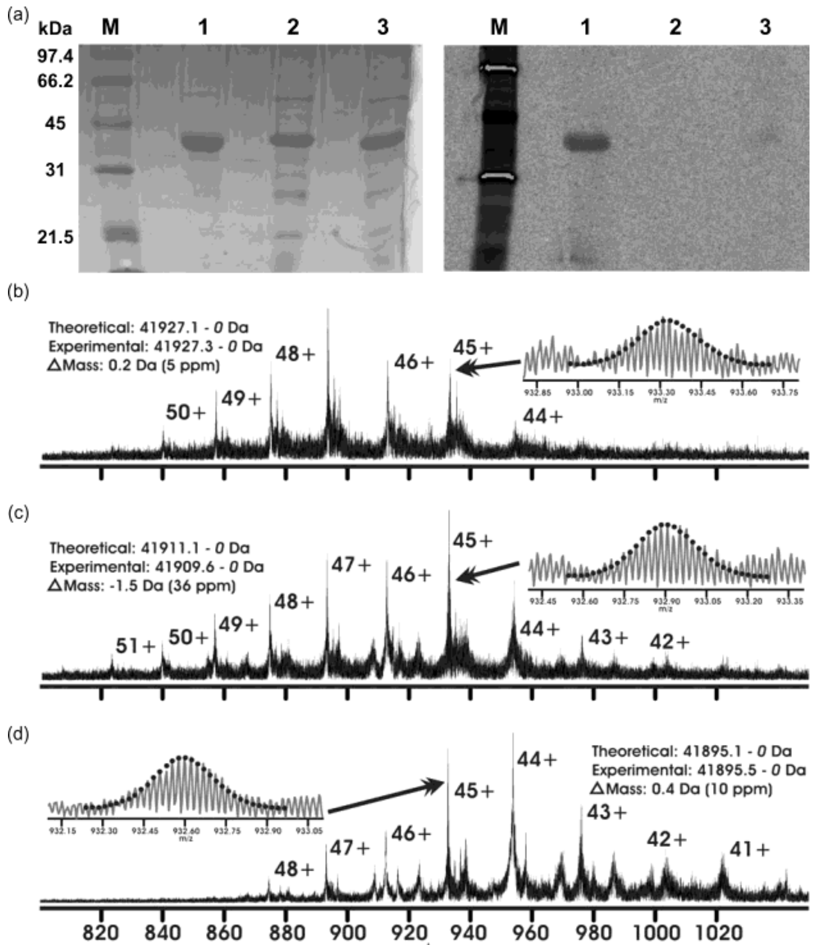

FIGURE 4: Dependence of the covalent labeling of DpgA with [^{14}C]-malonyl-CoA on Cys160. (a) Left side: Coomassie-stained 12% SDS−polyacrylamide gel of reaction mixtures. Right side: Autoradiograph of gel of same reaction mixtures. All reaction mixtures contained indicated wild-type or mutant DpgA (11.8 μM) and [^{14}C]-malonyl-CoA (35.4 μM, 10.2 Ci/mol). Lane 1, wild-type DpgA; lane 2, C160A; lane 3, C160S. M: molecular weight markers. (b) ESI−FTMS spectrum of wild-type DpgA consistent with the DNA-predicted sequence of DpgA without the start Met residue. (c) ESI−FTMS validation of the C160S mutant, 16 Da lower in mass than wild-type DpgA. (d) ESI−FTMS validation of the C160A mutant, 32 Da lower in mass than wild-type DpgA.

DpgB (1.8 μM) and DpgD (1.8 μM) at 24 °C (525 μL, pH 7.5). Ten 50-μL aliquots of the reactions were quenched with 900 μL of 10% trichloroacetic acid (TCA) over 90 min, with bovine serum albumin (200 μg) added as a carrier. The precipitated protein was washed three times with 900 μL of 10% TCA, and then dissolved in 150 μL of formic acid.

The amount of [^{14}C]-label incorporated was quantified by liquid scintillation counting. For time courses with the unlabeled malonyl-CoA chase, similar reaction conditions were used, except that total reaction volumes were 625 μL, and six aliquots were taken. Unlabeled malonyl-CoA (31.25 μL of 20 mM stock, or 1.44 mM) was added at 5.5 min. To compensate for the volume change, two 95-μL aliquots were taken before the addition of unlabeled malonyl-CoA and four 100-μL aliquots were taken after.

Autoradiography. [^{14}C]-Malonyl-CoA (35.4 μM, 10.2 Ci/mol) was incubated with wild-type or mutant DpgA (11.8 μM) at 24 °C (15 μL, pH 7.5) for 5 min. Reactions were quenched with gel-loading buffer and analyzed by SDS−PAGE (12%). The acrylamide gel was stained with Coomassie blue, destained, and dried on filter paper. The dried gel was exposed to a phosphorimager (Fuji, TR2040) for five days at 24 °C.

Activity Assays. Malonyl-CoA (5 mM) was incubated with wild-type or mutant DpgA (11 μM) either in the presence or absence of DpgB (33 μM) and DpgD (33 μM) at 24 °C (15 μL, pH 7.5) for 2 h. Reactions were quenched with 35 μL of 4% trifluoroacetic acid (TFA) and analyzed by HPLC using a Vydac C18 small pore column, monitoring at 258 nm (1 mL/min; 0−3 min, 0% B; 3−28 min, 0−50% B; A = H_2O, 0.1% TFA; B = acetonitrile; these conditions are used for all HPLC analysis of activity and kinetic assays). The product peak at 17.6 min was collected and subjected to matrix-assisted laser desorption ionization-time-of-flight mass spectrometry (MALDI-TOF MS) analysis. Similar reaction conditions were used for incubations of DpgB and DpgD with malonyl-CoA in the absence of DpgA.

Kinetic Analysis. To determine the kinetic parameters of wild-type DpgA on malonyl-CoA in the presence of DpgB and DpgD, increasing concentrations of malonyl-CoA were incubated with DpgA (50 nM), DpgB (150 nM), and DpgD (150 nM) at 24 °C (510 μL, pH 7.5). At 15 s and 20 min, 250-μL aliquots of the reactions were quenched with 50 μL of 4% TFA and analyzed by HPLC. The observed rates of increase of CoASH determined from the time courses were fit to the Michaelis−Menten equation to obtain values of k_{cat} and K_M. Similar reaction conditions were used to determine the kinetic parameters for the DpgA mutants, except for the C160A and C160A/H296A mutants, for which values of k_{cat}/K_M were obtained using Hanes-Woolf plots.

To determine the rates of acetyl-CoA and CoASH production by wild-type DpgA from malonyl-CoA in the presence of DpgB and DpgD, malonyl-CoA (5 mM) was incubated with DpgA (0.5 μM), DpgB (1.5 μM), and DpgD (1.5 μM) at 24 °C (50 μL, pH 7.5). At 15 s, 10 min, and 20 min, 15-μL aliquots of the reactions were quenched with 35 μL of 4% TFA and analyzed by HPLC, and the observed rates of increase of CoASH and acetyl-CoA were determined. Similar reaction conditions were used to determine the rates of acetyl-CoA and CoASH production by the DpgA mutants, and the rate of acetyl-CoA production by DpgB and DpgD in the absence of DpgA.

RESULTS

Radiolabeling of Wild-Type DpgA. We previously reported that incubations of DpgA with malonyl-CoA produced 3,5-dihydroxyphenylacetyl-CoA (DPA-CoA) and CoASH products, as analyzed by HPLC (*13*). Acetyl-CoA was also produced, presumably as the result of nonproductive decarboxylation of malonyl-CoA, but no other products were observed. Since derailment products could give us insight into the mechanism of action of DpgA [such products are released by RppA (*19*)], we examined whether any could be identified in the DpgA reaction by using [^{14}C]-malonyl-CoA as a substrate. None was detected, but we discovered that the enzyme itself was covalently radiolabeled to a 10−15% stoichiometric ratio by [^{14}C]-malonyl-CoA within several minutes, with the level of radiolabeling stable over a time scale of hours, as assessed by trichloroacetic acid precipitation (Figure 4a, data not shown).

The subsequent addition of excess unlabeled malonyl-CoA to the radiolabeled DpgA incubations resulted in the elimination of 40% of the enzyme-bound radiolabel within a few minutes (Figure 2). In the presence of DpgB and DpgD, a total of 80% of the radiolabel was removed over the same time scale (Figure 2). This chasing of the covalent radioactivity by molecules of unlabeled substrate indicates that the large majority of the radiolabel consists of one or more species on the reaction pathway. This is another demonstration of the importance of DpgB and DpgD in accelerating the rate of product formation by DpgA (*13*).

Mutations Eliminate Radiolabeling. To determine the location of the covalent radiolabel on DpgA, as well as to assess the roles of specific residues, five point mutants were made (Figure 3). The expected location of the radiolabel is on the catalytic Cys, which is identified by sequence alignments of type III polyketide synthase (PKS) enzymes to be Cys160, so this residue was mutated to either Ala or Ser. In addition, the predicted His residue of the catalytic triad, His296, was mutated to Ala, and the C160A/H296A double mutant was also constructed. Finally, a second Cys residue, Cys190, predicted to be in the active site based upon sequence alignments and the solved crystal structure of chalcone synthase (*14*), was also mutated to Ala. The identities of all of the mutants were confirmed at the DNA level by DNA sequencing, and the identities of the C160A and C160S mutants were also confirmed at the protein level by mass spectrometry (Figure 4c,d).

As expected, there was no detectable covalent radiolabeling of the C160A mutant, and the radiolabeling of the C160S mutant was reduced by 10-fold, consistent with lower levels of accumulating acyl-enzyme intermediates in the C160S mutant (Figure 4a). There was also no radiolabeling of the H296A and C160A/H296A mutants, supporting the importance of His296 for wild-type DpgA activity (data not shown). On the other hand, the C190A mutant was radiolabeled at wild-type levels, indicating that this residue is not relevant for enzymatic activity. Consistent with this conclusion, the radiolabel on the C190A mutant was chased away by unlabeled malonyl-CoA in a manner indistinguishable from that of wild-type DpgA (Figure 2).

Mutants Retain Product Formation Activity. In agreement with its wild-type levels of [^{14}C]-malonyl-derived radiolabeling, the C190A mutant displayed product formation activity similar to that of wildtype DpgA (Figure 5a). We were surprised to find, however, that although mutations of the Cys160 and His296 residues ablated detectable acyl-enzyme accumulation, as monitored by radiolabeling of DpgA, they did not fully eliminate product formation (Figure

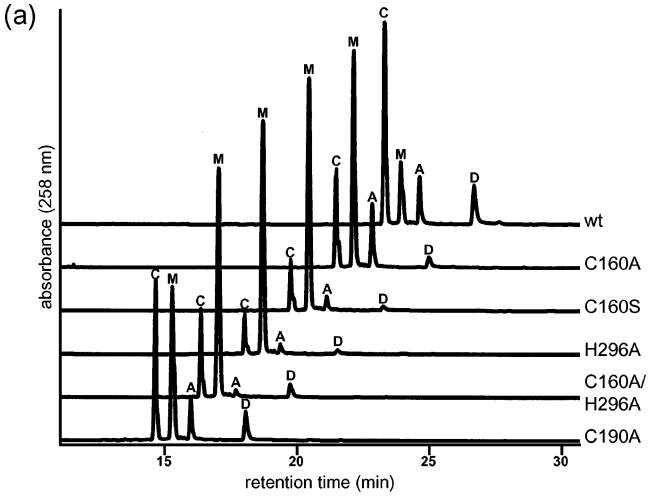

(b)

DpgA species	observed [M-H]$^-$ of DPA-CoA (calculated [M-H]$^-$ = 916.2)
wt	915.9
C160A	916.0
C160S	916.1
H296A	916.2
C160A/H296A	916.2
C190A	916.1

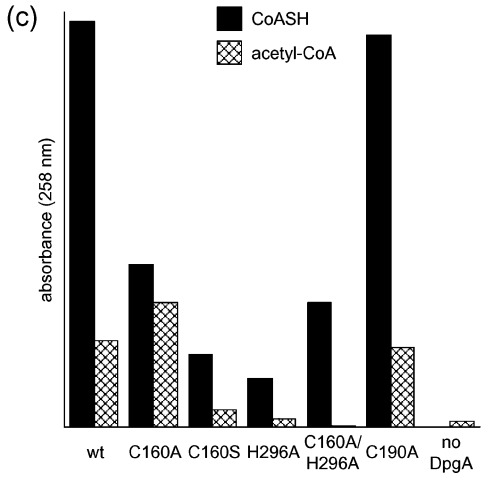

FIGURE 5: Catalytic activities of DpgA mutants. (a) HPLC traces of 2 h reactions initially containing 5 mM malonyl-CoA, 11 μM indicated wild-type or mutant DpgA, 33 μM DpgB, 33 μM DpgD, and 50 mM Tris, at pH 7.5 and 24 °C. The peaks corresponding to CoASH (C), malonyl-CoA (M), acetyl-CoA (A), and DPA-CoA (D) are labeled. For clarity, traces are offset from one another by 2 min. (b) MALDI-TOF MS characterization of DPA-CoA peaks from HPLC traces in panel a. (c) Relative absorbances of CoASH and acetyl-CoA peaks from HPLC traces in panel a, and from trace of analogous reaction without DpgA.

5). These results diverge from those for other type III PKSs characterized to date, including chalcone synthase and RppA (*19*, *20*), in which point mutants of either the catalytic Cys or His are completely incompetent for product formation. This suggests that either another residue can substitute for the catalytic Cys in acyl-enzyme intermediate formation, or that the formation of covalent intermediates is not necessary for this enzyme (see Discussion). In particular, the possibility of small thiol molecules, such as dithiothreitol (DTT), acting as carriers for noncovalent intermediates was investigated by substituting tris(2-carboxyethyl)phosphine hydrochloride for DTT in the dialysis buffer of the enzymes. This substitution was found to have no effect on enzyme activity, arguing against the utility of small thiols as carriers (data not shown).

The products formed by all of the DpgA mutants were confirmed to be DPA-CoA by HPLC co-chromatography, as well as by mass spectrometry (Figure 5a,b). Detection of product formation by the DpgA mutants was completely dependent upon the presence of DpgB and DpgD (data not shown). Interestingly, these two enzymes were also observed to have the ability to decarboxylate malonyl-CoA to acetyl-CoA at a low rate above background when incubated together, but not individually, with malonyl-CoA in the absence of DpgA (Figure 5c).

Kinetic parameters were determined for the C160A and C160S mutants, using the reasoning that four malonyl-CoA substrate molecules result in three CoASH and one DPA-CoA product molecules to obtain turnover data (Scheme 1, Figure 6). The ratio of DPA-CoA to CoASH produced by both mutants was the same as for wild-type DpgA, confirming the validity of this reasoning (Figure 5a, data not shown). The C160A mutant had significantly different kinetic parameters from those of wild-type DpgA, most notably in its K_M for malonyl-CoA. Severe substrate inhibition was observed at malonyl-CoA concentrations above 5 mM, at which point the Michaelis−Menten curve of the C160A mutant did not yet show signs of saturation (Figure 6a), so the K_M of this mutant was significantly greater than 300-fold that of wild-type DpgA. At this maximal substrate concentration, the k_{cat} of the C160A mutant was already 50% of that of wild-type DpgA. We measured the overall catalytic efficiency (k_{cat}/K_M) of the C160A mutant to be 500-fold lower than that of wild-type DpgA. The C160S mutant had a less drastic change in kinetic parameters relative to wild-type DpgA, with a 5-fold lower k_{cat} and 10-fold greater K_M, resulting in a 50-fold reduced k_{cat}/K_M (Figure 6b). The K_M values for the H296A and C190A mutants were comparable to that of wild-type, while the C160A/H296A double mutant displayed similar kinetic parameters to the C160A mutant (data not shown). Also, the k_{cat} for the H296A mutant was reduced only one order of magnitude, a surprisingly robust rate when the proposed catalytic residue for decarboxylation of the malonyl-CoA substrate is removed (Figure 5a, data not shown).

C160A Mutant Has Increased Unproductive Acetyl-CoA Formation. In addition to having altered kinetic parameters relative to wild-type DpgA, the C160A mutant also produced significantly more acetyl-CoA relative to DPA-CoA product, indicating a greater amount of nonproductive decarboxylation of malonyl-CoA (Figure 7). In fact, 40% of the malonyl-CoA substrate was partitioned toward unproductive acetyl-CoA in the C160A mutant, as compared with 23% for wild-type DpgA. On the other hand, the C160S mutant showed comparable substrate partitioning to wild-type DpgA, with 27% of the substrate producing dead-end acetyl-CoA instead of becoming incorporated into DPA-CoA product (Figure 7). Of these partition percentages, 3% can be attributed to the low rate of DpgA-independent malonyl-CoA decarboxylation catalyzed by DpgB and DpgD (Figure 5c, data not shown).

(a)

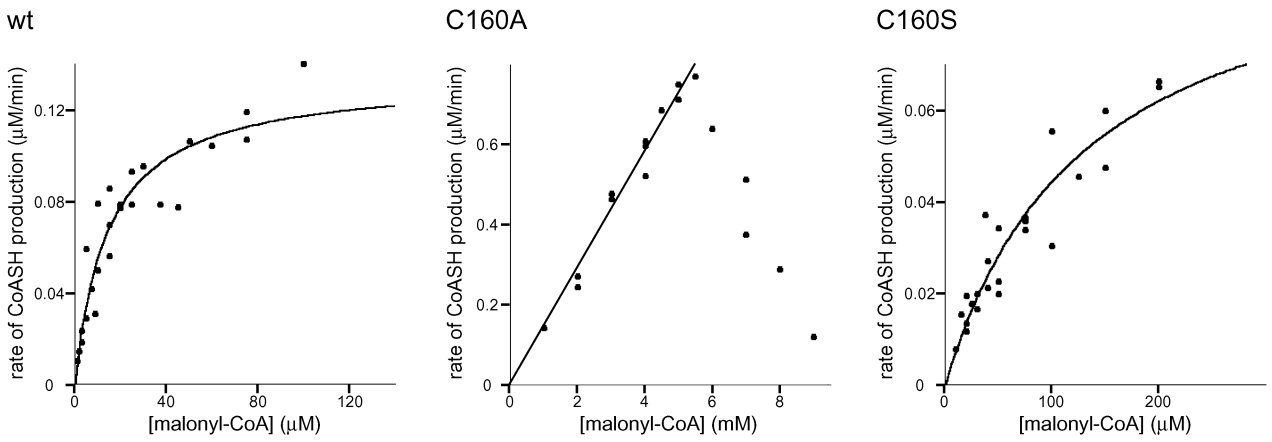

(b)

	k_{cat} (min^{-1})	relative k_{cat}	K_M (μM)	relative K_M	k_{cat}/K_M (mM^{-1}min^{-1})	relative k_{cat}/K_M
wt	0.81 ± 0.05	1	15 ± 3	1	55	1
C160A	>0.41 ± 0.05	>0.51	>5000	>330	0.091	0.0016
C160S	0.171 ± 0.002	0.21	130 ± 40	9.1	1.3	0.023

FIGURE 6: Characterization of Cys160 mutants. (a) Michaelis−Menten curves for CoASH production by wild-type, C160A, and C160S DpgA. Curve for C160A mutant includes malonyl-CoA concentrations below 5 mM, above which severe substrate inhibition is observed. (b) Absolute and relative k_{cat} and K_M values of DPA-CoA formation by wild-type, C160A, and C160S DpgA.

(a)

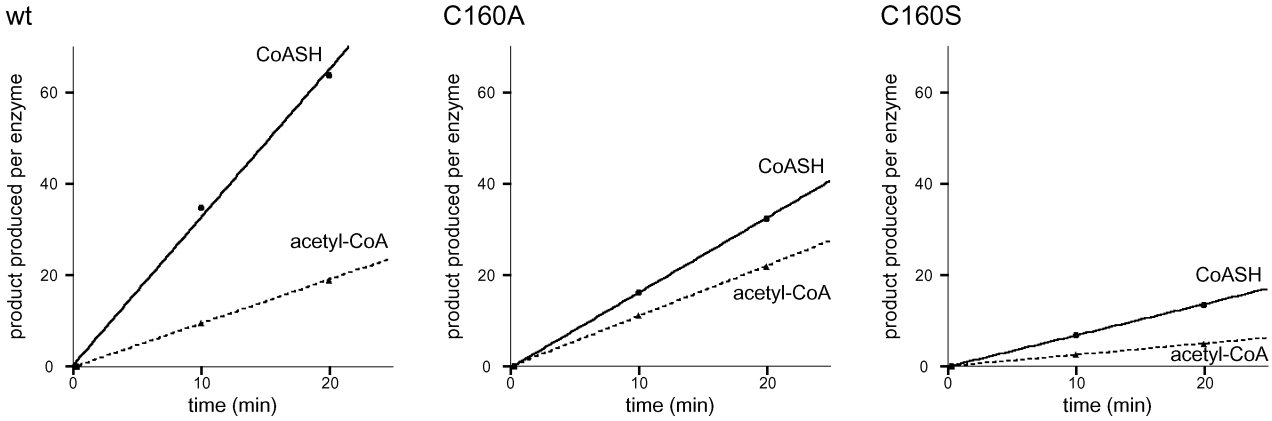

(b)

	k_{cat} CoASH (min^{-1})	relative k_{cat} CoASH	k_{cat} acetyl-CoA (min^{-1})	relative k_{cat} acetyl-CoA	partition of substrate to acetyl-CoA
wt	3.2 ± 0.2	1	0.96 ± 0.01	1	23%
C160A	>1.6 ± 0.2	>0.51	>1.1 ± 0.1	>1.2	40%
C160S	0.68 ± 0.01	0.21	0.25 ± 0.01	0.26	27%

FIGURE 7: Characterization of unproductive acetyl-CoA formation by Cys160 mutants. (a) Initial rates of CoASH and acetyl-CoA production by wild-type, C160A, and C160S DpgA in reactions initially containing 5 mM malonyl-CoA. (b) Absolute and relative k_{cat} and K_M values of CoASH and acetyl-CoA formation by wild-type, C160A, and C160S DpgA.

DISCUSSION

The bacterial type III polyketide synthase (PKS) enzyme DpgA is of interest for several reasons. First, it is the gatekeeper enzyme for shunting the primary metabolite malonyl-CoA to a nonproteinogenic amino acid, the eight-carbon aromatic 3,5-dihydroxyphenylglycine (Dpg). Dpg is the seventh residue in the heptapeptide backbone of vancomycin and teicoplanin, and its electron-rich aromatic side chain undergoes crucial oxidative cross-linking to the 4-hydroxyphenylglycine$_5$ side chain to set the architecture required for recognition of bacterial cell wall peptidoglycan termini (*9*). Second, DpgA takes four identical malonyl-CoA substrates, makes four C−C bonds, and controls the regiochemistry of cyclization in the last step to create an unusual

Scheme 2: Alternate Mechanisms of Action of DpgA[a]

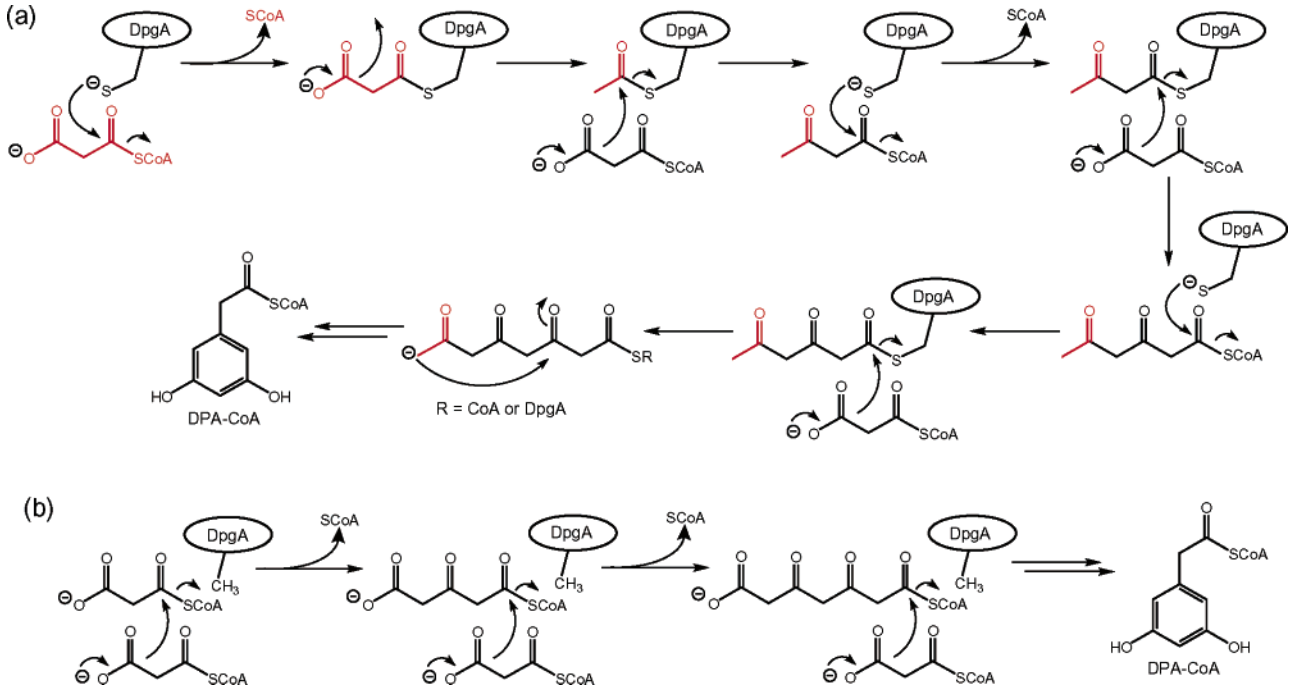

[a] (a) Mechanism of action if starter malonyl-CoA substrate, indicated in red, is decarboxylated after loading onto active site Cys instead of concomitantly with cyclization. (b) Mechanism of action with noncovalent intermediates.

C_8 to C_3 linkage as prelude to aromatization. A comparable reaction by the type I PKS CalO5 in calicheamicin biosynthesis or AviM in avilamycin biosynthesis generates the eight-carbon aromatic acid orsellinic acid, but with a C_2 to C_7 cyclization mode (*21*, *22*).

C−C bond formations that proceed via controlled decarboxylations of malonyl thioesters attacking electrophilic carbonyl centers represent classic fatty acid synthase and PKS biosynthetic logic (*23*, *24*). Type III PKS enzymes are defined as utilizing acyl-CoA thioester substrates rather than the acyl-ACP thioester substrates of type I and II PKSs, so DpgA is thereby classified as a type III PKS. This PKS subfamily is most prevalent in plants, where chalcone synthases, for example, initiate entry into flavonoid pathways of secondary metabolism (*14*). Most of the plant type III PKSs use an electrophilic starter acyl-CoA, and engage in one to three cycles of elongation with malonyl-CoAs acting as nucleophilic extender units before a chain-terminating cyclization occurs. Bacterial type III PKS systems have been identified through genomics efforts, with the first member discovered, RppA, catalyzing five cycles of malonyl-CoA condensation to tetrahydroxynaphthalene (*15*). Bacterial RppA and DpgA use malonyl-CoA as both electrophilic starter and nucleophilic extender units, so the differentiation of function is a mechanistic and specificity issue, as is the timing of decarboxylation of the first vs subsequent malonyl-CoA units to control their reactivity as carbon nucleophiles.

The prototypic mechanism for type III PKS condensing enzymes and the evolutionarily related type III ketosynthases of fatty acid assembly (*14*) is the use of an obligately conserved active site Cys as an initiating nucleophile on the starter acyl-CoA substrate to form an acyl-*S*-Cys-enzyme covalent intermediate. This is then the electrophilic partner in the first C−C bond-forming step, driven by decarboxylation of the first extender malonyl-CoA to generate the requisite carbon nucleophile (Scheme 1). The coupled decarboxylation/C−C condensation is mediated by a conserved active site His to initiate the decarboxylation once the active site Cys is acylated. This coupling transfers the loaded acyl group onto the acetyl-CoA enolate, producing an elongated β-ketoacyl-CoA and the free active site Cys thiolate. To engage in the next cycle of elongation, it has been presumed that transthiolation occurs: the chain-extended β-ketoacyl-*S*-enzyme is formed, clearing space for binding of the next malonyl-CoA. Iterative condensations then shuttle the elongating acyl chain between the active site Cys thiolate and the nascent C_2-carbanion of acetyl-CoA, arising from decarboxylation of bound malonyl-CoA. The active site Cys and His, Cys160 and His296 in DpgA by sequence homology, participate in every elongation cycle, three in DpgA and four in RppA.

Among the fundamental questions of such reciprocating mechanisms for C−C bond formation are the timing of malonyl-CoA decarboxylation, the orientation and placement of the electrophilic and nucleophilic partner chains in each condensation cycle, and the regiochemistry of product control by such enzymatic assembly lines (*14*). The timing of decarboxylation of the first malonyl-CoA unit could happen after transfer to the active site Cys thiolate and before C−C bond formation to give acetyl-*S*-Cys-enzyme, which would be competent only as the electrophilic partner in subsequent condensations (Scheme 2a). Then, the series of chain elongations would yield C_2, C_4, and C_6 acyl chains covalently tethered to the enzyme. The last condensation would yield a C_8 tetraketidyl-*S*-CoA, which could either form the C_8 acyl-*S*-enzyme or be cyclized prior to such a transthiolation step. Alternatively, the C_3-carboxylate of the first malonyl-CoA could be retained all the way through the iterative cycles of elongation, to yield C_3, C_5, C_7, and C_9 acyl chains (Scheme 1).

Scheme 3: Hypothetical Reaction Coordinate of Conversion of four Malonyl-CoA Molecules to DPA-CoA by DpgA[a]

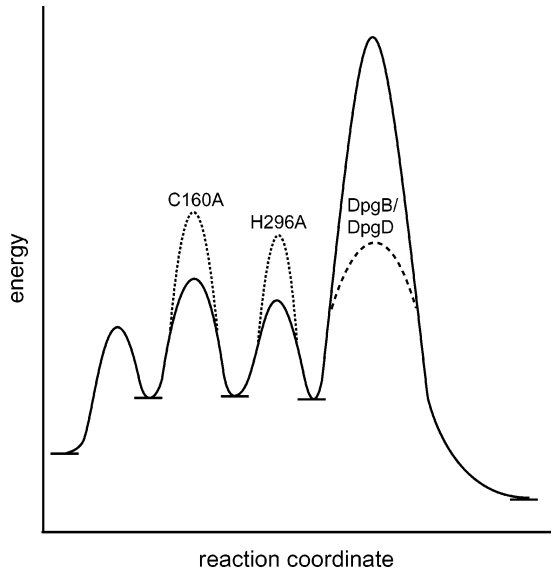

[a] In this schematic, the rate-determining step is release of final product, which is the step proposed to be chaperoned by DpgB and DpgD, as shown by the dashed line. Under such conditions, it is possible that mutations affecting previous steps, with two hypothetical examples shown by the dotted lines, would not have a significant effect on the overall reaction rate.

The question then arises if covalent acyl-*S*-enzyme intermediates can be detected during catalytic turnover, and, if so, what species accumulate (C_2, C_3, C_4, C_5, C_6, C_7, C_8, and C_9 acyl chains are possible, as noted in Schemes 1 and 2a). With wild-type DpgA, [^{14}C]-malonyl-CoA leads to covalent labeling of the enzyme up to 15% of stoichiometry when subjected to acid quench during turnover. While such studies are a preamble to rapid quench experiments to deconvolute the time course through a single catalytic cycle, they do establish that the anticipated covalent catalysis is operating. In principle, up to 4 equivalents of [^{14}C]-malonyl radioactivity could be on the enzyme if a C_8 or C_9 acyl-*S*-enzyme intermediate accumulated on 100% of the DpgA molecules during turnover. On the other hand, the reciprocating mechanism of type III PKSs predicts that every other intermediate is at least transiently not covalently associated while in the acyl-CoA form. Such intermediates could diffuse away from the active site and not be detectable as acyl-*S*-enzyme forms. The identity and distribution of the 0.15 covalent acyl groups, between C_2 and C_9, on the enzyme have not yet been determined for DpgA or any other type III PKS. In pulse chase studies, about 40% of the [^{14}C]-malonyl-derived covalent label could be chased off DpgA by unlabeled malonyl-CoA in the absence of DpgB and DpgD. Inclusion of DpgB and DpgD resulted in an 80% chase, consistent with these proteins accelerating a slow release step (Scheme 3) and validating that most of the [^{14}C]-malonyl-derived radioactivity incorporated onto DpgA is on the catalytic pathway.

Assaying purified DpgA with [^{14}C]-malonyl-CoA also allows for monitoring the release of any of the putative intermediates [the C_4, C_6, C_8, or the corresponding C_5, C_7, C_9 linear di-, tri-, and tetraketidyl-CoAs (Schemes 1 and 2a)] that might diffuse away from the active site during catalytic turnover. No such radioactive intermediate fragments or derivative lactones, e.g., triacetic lactone (*25*), were detected, suggesting that the enzyme holds onto such acyl-CoAs tightly and/or they have very short lifetimes before recapture by the active site Cys thiolate.

The amount of DpgA that accumulates in covalent acyl-enzyme forms drops an order of magnitude when the Cys160-thiolate is replaced by a hydroxyl in the C160S mutant, and drops to negligible levels when the nucleophilic side chain is removed and replaced by a methyl in the C160A mutant. The failure to see any [^{14}C]-acyl-enzyme in the Ala mutant is as expected, and is consistent with the attachment of [^{14}C]-acyl groups in wild-type DpgA on the active site Cys side chain. To rule out the possibility that Cys190, a second Cys predicted to be in the active site (*14*), might instead be the catalytic nucleophile, it was mutated to Ala, and the C190A mutant had the same activity as wild-type DpgA.

The only radioactive species detected in solution other than product DPA-CoA was [^{14}C]-acetyl-CoA. In principle, if every decarboxylation of malonyl-CoA (or malonyl-*S*-enzyme) was completely coupled to C−C bond formation in the three elongations and final cyclization step, there should be no acetyl-CoA released. In fact, about one acetyl-CoA was produced for every complete DPA-CoA product in incubations yielding thousands of turnovers, so there is 20% uncoupling: decarboxylation of malonyl-CoA that is unproductive, either in timing or locale, such that the acetyl-CoA enolate reprotonates to acetyl-CoA rather than acts as a carbon nucleophile. It is likely that the DpgA active site is not configured to deprotonate acetyl-CoA molecules and allow them back into the catalytic flux, since mixtures of malonyl-CoA and [^{14}C]-acetyl-CoA yield no radioactive DPA-CoA (*13*). The canonical type III PKS schemes (*14*, *26*), e.g., Scheme 1, have the malonyl-CoA extender units being decarboxylated while not covalently attached to the active site Cys, consistent with the idea that if the C_2 carbanion is quenched with a proton rather than a C−C bond formation, the resultant acetyl-CoA can diffuse out of the active site and be replaced by another malonyl-CoA without interruption of the catalytic cycle. Thus, 20% acetyl-CoA formation during catalysis indicates 20% inefficiency in catalytic flux, with, on average, one in five malonyl-CoAs decarboxylated prematurely in the DpgA active site. When the C160A and C160S mutants were examined, the inefficiency had risen to 37 and 24%**,** respectively, consistent with some modest increased disruption in the orderly flow of the many intermediates in this C−C bond-forming factory.

The Cys160 mutants of DpgA allow insight into the central tenet of the type III PKS mechanism, in which the acyl chain is installed on the thiolate of the active site Cys. C−C bond formation and chain elongation move the chain from the active site Cys onto the nascent acetyl-CoA enolate. Chain translocation of the elongated β-ketoacyl chain back onto the active site Cys is prelude to binding the next extender malonyl-CoA and setting up its triggered decarboxylation to repeat the elongation cycles. When the C160A mutant of DpgA was prepared, we expected that covalent [^{14}C]-malonylation would disappear, as it did. We anticipated that unproductive malonyl-CoA decarboxylation activity might thereby rise, as it did. We did not, however, anticipate that the C160A mutant form of DpgA would be functional in turnover, but it clearly was. We validated the Ala mutation

at both the DNA and protein level, and the two aforementioned observations, failure to give covalent [^{14}C]-malonyl-enzyme and increased decarboxylation ratios, accord with the mutant nature of the active site.

The C160A mutant of DpgA still turns over malonyl-CoA to DPA-CoA at up to 50% of V_{max}, although catalytic efficiency is reduced 500-fold. DPA-CoA was characterized as authentic product by HPLC co-chromatography and mass spectrometry. There were still no partially elongated intermediates released, as though essential rate-determining steps had not changed, and the required chaperoning of DpgB and DpgD to release DPA-CoA was still operant (Scheme 3). Clearly, although the wild-type enzyme makes [^{14}C]-acyl-*S*-Cys-enzyme intermediates, it can still make the eight-carbon DPA-CoA product if deprived of the catalytic nucleophile (and the presumed catalytic base for malonyl decarboxylation, His296, both singly and in combination). One possible mechanism is that an alternate nucleophile takes over from Cys160 in the enzyme active site, but if so, its accumulation as a [^{14}C]-acyl-enzyme drops precipitously to unmeasurable levels while still carrying up to 50% of the wild-type flux. Perhaps more likely is that the C−C bond-forming steps in the C160A mutant of DpgA occur between two bound acyl-CoAs (e.g., two malonyl-CoAs form a C_5-acyl-CoA, which, in turn, gives a C_7 and C_9-acyl-CoA) (Scheme 2b). The thermodynamic activation of the two substrate partners as thioesters would be retained as in wild-type enzyme. What would be unanticipated in this path is that there would be room for two large CoA-moieties on the enzyme in or near the active site, given the structural precedents for type III PKSs whose structures have been solved and acyl-CoA binding sites mapped (*26*, *27*). It also does not appear, however, that small solution thiol molecules, such as dithiothreitol, are acting as carriers for such non-covalent intermediates, given that tris(2-carboxyethyl)phosphine hydrochloride can substitute for these buffer thiols.

Finally, there is the question of how disabling the catalytic machinery, Cys160 and/or His296, of this type III PKS could lead to only a 10- to 20-fold drop in turnover rates. This touches upon the curious roles of DpgB and DpgD in accelerating the flux of acyl-enzyme intermediates and product release. We have earlier (*13*) noted that each has crotonase type activity, and have speculated that one or both could be dehydrating the intial cyclic adduct as the CoA-thioester or as the Cys160-thioester in the DpgA active site. The corresponding aromatizations by chalcone synthase and RppA, which do not include the unusual C_8 to C_3 cyclization that DpgA does, have been assumed to be uncatalyzed (*15*, *26*). Understanding the remarkable iterative elongation logic of type III PKS machinery will require identification of the distribution of the accumulating acyl-*S*-enzyme intermediates and structure determination of the active mutants with bound ligands.

ACKNOWLEDGMENT

We thank members of the Walsh lab for helpful discussions.

REFERENCES

1. van Wageningen, A. M. A., Kirkpatrick, P. N., Williams, D. H., Harris, B. R., Kershaw, J. K., Lennard, N. J., Jones, M., Jones, S. J. M., and Solenberg, P. J. (1998) Sequencing and analysis of genes involved in the biosynthesis of a vancomycin group antibiotic. *Chem. Biol. 5*, 155−162.
2. Pelzer, S., Sü*β*muth, R., Heckmann, D., Recktenwald, J., Huber, P., Jung, G., and Wohlleben, W. (1999) Identification and analysis of the balhimycin biosynthetic gene cluster and its use for manipulating glycopeptide biosynthesis in *Amycolatopsis mediterranei* DSM5908. *Antimicrob. Agents Chemother. 43*, 1565−1573.
3. Chiu, H.-T., Hubbard, B. K., Shah, A. N., Eide, J., Fredenburg, R. A., Walsh, C. T., and Khosla, C. (2001) Molecular cloning and sequence analysis of the complestatin biosynthetic gene cluster. *Proc. Natl. Acad. Sci. U.S.A. 98*, 8548−8553.
4. Sosio, M., Stinchi, S., Beltrametti, F., Lazzarini, A., and Donadio, S. (2003) The gene cluster for the biosynthesis of the glycopeptide antibiotic A40926 by *Nonomuraea* species *Chem. Biol. 10*, 541−549.
5. Pootoolal, J., Thomas, M. G., Marshall, C. G., Neu, J. M., Hubbard, B. K., Walsh, C. T., and Wright, G. D. (2002) Assembling the glycopeptide antibiotic scaffold: the biosynthesis of A47934 from *Streptomyces toyocaensis* NRRL15009. *Proc. Natl. Acad. Sci. U.S.A. 99*, 8962−8967.
6. Walsh, C. T. (2002) Combinatorial biosynthesis of antibiotics: challenges and opportunities. *Chembiochem 3*, 124−134.
7. Stein, T., Vater, J., Kruft, V., Otto, A., Wittman-Liebold, B., Franke, P., Panico, M., McDowell, R., and Morris, H. R. (1996) The multiple carrier model of nonribosomal peptide biosynthesis at modular multienzymatic templates. *J. Biol. Chem. 271*, 15428−15435.
8. Walsh, C. T., Chen, H., Keating, T. A., Hubbard, B. K., Losey, H. C., Luo, L., Marshall, C. G., Miller, D. A., and Patel, H. M. (2001) Tailoring enzymes that modify nonribosomal peptides during and after chain elongation on NRPS assembly lines. *Curr. Opin. Chem. Biol. 5*, 525−534.
9. Hubbard, B. K., and Walsh, C. T. (2003) Vancomycin assembly: nature's way. *Angew. Chem. Int. Ed. 42*, 730−765.
10. Hubbard, B. K., Thomas, M. G., and Walsh, C. T. (2000) Biosynthesis of L-*p*-hydroxyphenylglycine, a non-proteinogenic amino acid constituent of peptide antibiotics. *Chem. Biol. 7*, 931−942.
11. Choroba, O. W., Williams, D. H., and Spencer, J. B. (2000) Biosynthesis of the vancomycin group of antibiotics: involvement of an unusual dioxygenase in the pathway to (*S*)-4-hydroxyphenylglycine. *J. Am. Chem. Soc. 122*, 5389−5390.
12. Pfeifer, V., Nicholson, G. J., Ries, J., Recktenwald, J., Schefer, A. B., Shawky, R. M., Schröder, J., Wohlleben, W., and Pelzer, S. (2001) A polyketide synthase in glycopeptide biosynthesis: the biosynthesis of the non-proteinogenic amino acid (*S*)-3,5-dihydroxyphenylglycine. *J. Biol. Chem. 276*, 38370−38377.
13. Chen, H., Tseng, C. C., Hubbard, B. K., and Walsh, C. T. (2001) Glycopeptide antibiotic biosynthesis: enzymatic assembly of the dedicated amino acid monomer (*S*)-3,5-dihydroxyphenylglycine. *Proc. Natl. Acad. Sci. U.S.A. 98*, 14901−14906.
14. Austin, M. B., and Noel, J. P. (2003) The chalcone synthase superfamily of type III polyketide synthases. *Nat. Prod. Rep. 20*, 79−110.
15. Funa, N., Ohnishi, Y., Fujii, I., Shibuya, M., Ebizuka, Y., and Horinouchi, S. (1999) A new pathway for polyketide synthesis in microorganisms. *Nature 400*, 897−899.
16. Ho, S. N., Hunt, H. D., Horton, R. M., Pullen, J. K., and Pease, L. R. (1989) Site-directed mutagenesis by overlap extension using the polymerase chain reaction. *Gene 77*, 51−59.
17. Senko, M. W., Hendrickson, C. L., Emmett, M. R., Shi, S. D.-H., and Marshall, A. G. (1997) External accumulation of ions for enhanced electrospray ionization Fourier transform ion cyclotron resonance mass spectrometry. *J. Am. Soc. Mass Spectrom. 8*, 970−976.
18. Kelleher, N. L., Lin, H. Y., Valaskovic, G. A., Aaserud, D. J., Fridriksson, E. K., and McLafferty, F. W. (1999) Top down versus bottom up protein characterization by tandem high-resolution mass spectrometry. *J. Am. Chem. Soc. 121*, 806−812.
19. Funa, N., Ohnishi, Y., Ebizuka, Y., and Horinouchi, S. (2002) Alteration of reaction and substrate specificity of a bacterial type III polyketide synthease by site-directed mutagenesis. *Biochem. J. 367*, 781−789.
20. Jez, J. M., Ferrer, J.-L., Bowman, M. E., Dixon, R. A., and Noel, J. P. (2000) Dissection of malonyl-coenzyme A decarboxylation from polyketide formation in the reaction mechanism of a plant polyketide synthase. *Biochemistry 39*, 890−902.

21. Ahlert, J., Shepard, E., Lomovskaya, N., Zazopoulos, E., Staffa, A., Bachmann, B. O., Huang, K., Fonstein, L., Czisny, A., Whitwam, R. E., Farnet, C. M., and Thorson, J. S. (2002) The calicheamicin gene cluster and its iterative type I enediyne PKS. *Science 297*, 1173−1176.
22. Gaisser, S., Trefzer, A., Stockert, S., Kirschning, A., and Bechthold, A. (1997) Cloning of an avilamycin biosynthetic gene cluster from *Streptomyces viridochromogenes* Tü57. *J. Bacteriol. 179*, 6271−6278.
23. Rawlings, B. J. (1998) Biosynthesis of fatty acids and related metabolites. *Nat. Prod. Rep. 15*, 275−308.
24. Rawlings, B. J. (1997) Biosynthesis of polyketides. *Nat. Prod. Rep. 14*, 523−556.
25. Funa, N., Ohnishi, Y., Ebizuka, Y., and Horinouchi, S. (2002) Properties and substrate specificity of RppA, a chalcone synthase-related polyketide synthase in *Streptomyces griseus*. *J. Biol. Chem. 277*, 4628−4735.
26. Ferrer, J.-L., Jez, J. M., Bowman, M. E., Dixon, R. A., and Noel, J. P. (1999) Structure of chalcone synthase and the molecular basis of plant polyketide biosynthesis. *Nat. Struct. Biol. 6*, 775−784.
27. Jez, J. M., Austin, M. B., Ferrer, J.-L., Bowman, M. E., Schröder, J., and Noel, J. P. (2000) Structural control of polyketide formation in plant-specific polyketide synthases. *Chem. Biol. 7*, 919−930.

BI035714B